



IJRASET

International Journal For Research in
Applied Science and Engineering Technology



INTERNATIONAL JOURNAL FOR RESEARCH

IN APPLIED SCIENCE & ENGINEERING TECHNOLOGY

Volume: 8 Issue: X Month of publication: October 2020

DOI: <https://doi.org/10.22214/ijraset.2020.32014>

www.ijraset.com

Call:  08813907089

E-mail ID: ijraset@gmail.com

Synthesis and Characterization of $\text{La}_x\text{Zn}_{1-x}\text{Fe}_2\text{O}_4$ ($x = 0.0 \leq x \leq 0.3$) Nanoparticles by Sol-Gel Self-Ignition Method

D. Nandhini¹, D. Keerthana²

¹Assistant Professor in, Department of Physics, Prist Deemed to be University, Thanjavur, Tamilnadu

²M.phil Scholar, Department of Physics, Prist Deemed to be University, Thanjavur, Tamilnadu

Abstract: Review of literature is a comprehensive and extensive of several research works done by many researches on a selected field. The survey of part and ongoing research on ferrites nanoparticles will give better understanding of the preparation of materials and its synthesis and characterization.

Oana Mihai et al. [1] have synthesized cubic LaFeO_3 nanoparticles using carbon nanotubes as templates. Samples were characterized by high surface area ($30 \text{ m}^2 \text{ g}^{-1}$) have been synthesized, which are stable at high temperatures up to 1173 K. Carbon nanotubes (CNTs) were used as hard templates. The advantages of this synthesis are evidenced in this study by comparing the phase, size and stability of the resulting LaFeO_3 perovskite with those synthesized by using the well-established citrate method. CNTs can stabilize not only the perovskite cubic structure, but also the size.

Keywords: Synthesis & Characterization, Nonopaticles, Sol-gel, Self-Ignition method

I. INTRODUCTION

A. Nanoscience

Study on fundamental relationship between physical properties and material dimensions in the nanoscale are called "Nanoscience". Nanoscience is the study of phenomena and manipulation of materials at atomic, molecular and macromolecular scales, where properties differ significantly from those at a larger scale. Nanoscience is an emerging area of science, which concerns itself with the study of materials that have very-very small dimensions [1]. Nanoscience is usually defined as science at a nanoscale, which is fairly flexible definition, and could include materials up to the 1000 nm scale, although it is normally regarded as scales up to 10-100 nm.

II. EXPERIMENTAL TECHNIQUES

A. Top-Down Approaches

Methods to produce nanoparticles from bulk materials include high energy ball-milling, mechano-chemical processing, etching, electro explosion, sonication, sputtering and laser-ablation. These processes are done in an inert atmosphere or in vacuum.

B. Bottom-Up Approaches

The chemical methods of producing semiconductor nanoparticles can be divided into four categories. The colloidal route, organic metallic route, growth-in-confined matrices and gas phase synthesis of nanoparticles out of which aqueous colloidal precipitation route is optimized for the precipitation of doped ZnO nanocrystals. Due to their high reactivity nanoparticles have a high tendency to build aggregates respectively agglomerates, which could lead to a loss of the desired properties. Therefore it is often necessary to stabilize the nanoparticles with additional treatments. Stabilization mechanism of nanoparticles can be categorized as, [1]

C. Aerosol Synthesis

Aerosol method is a top-down approach for synthesis of polycrystalline nanoparticles. In this method, the liquid precursor which is a simple mixture of the desired constituent element (or) colloidal dispersion is mystified to make liquid aerosol. The liquid aerosol is a dispersion of uniform droplets of liquid in a gas which may simply solidified through evaporation of solvent (or) further reacts with the chemicals that are present in the gas. The resulting particles are spherical and their size is determined by the size of the initial liquid droplets and concentration of the solid. This method can also use to prepare the polymer colloids.

D. Sol-Gel Processing

The sol-gel process is a solution phase processing technique that is used more often to fabricate nanostructured materials. This is a process capable of producing nanostructured ceramics and composites. It involves the evolution of networks through the formation of colloidal suspension (sol) and gelatin to form a network in continuous liquid phase (gel). The precursor for synthesizing these colloids consists of ions of metal alkoxides and aloxysilanes. The most widely used are tetramethoxysilane (TMOS), and tetraethoxysilane (TEOS) which form silica gels. Alkoxides are immiscible in water. Alcohol can be used as a mutual solvent. A catalyst is used to start reaction and the pH is controlled. Sol-gel formation occurs in four stages.

- 1) Hydrolysis.
- 2) Condensation.
- 3) Growth of particles.
- 4) Agglomeration of particles [6].

E. Hydrolysis Process

The simple oxides are produced by precipitation process by adding a mineralizing agent. The co-precipitation process is utilized for synthesis of mixed oxides. The advantages of these processes are: the accessibility of precursors and the homogeneity of chemical composition. The agglomeration of powders and the simultaneous co-precipitation of all cations from solution are the main disadvantage of hydrolysis method.

F. Chemical Vapour Condensation

This process involves the pyrolysis of vapour of metal organic precursors in a reduced atmospheric pressure. A metal organic precursor is introduced in the hot zone of the reactor using mass flow controllers. The reactor allows synthesis of mixtures of nanoparticles of two phases or doped nanoparticles by supplying two precursors at the front end of reactor and coated nanoparticles by supplying a second precursor in a second stage of reactor. The process yields quantities in excess of 20g/hr. the yield can be further improved by enlarging the diameter of not wall reactor and mass of fluid through the reactor.

G. Sonochemical Process

In sonochemical process nanoparticles are generated through creation and release of gas bubbles inside the sol-gel solution. By exposing to cavitation disturbances and high temperature heating, the hydrodynamic bubbles are erupted. This causes the nucleation, growth and quenching of nanoparticles, particle size can be controlled by adjusting pressure and solution retention times. [7]

H. Self Propagating Method

Self-propagating low-temperature synthesis is a method for producing [inorganic compounds](#) by exothermic reactions, usually involving salts. A variant of this method is known as solid state metathesis (SSM). Since the process occurs at low temperatures, the method is ideally suited for the production of refractory materials with unusual properties, for example: powders, metallic alloys, or ceramics with high purity, corrosion-resistance at high-temperature.

In its usual format, SLS is conducted starting from finely powdered reactants that are intimately mixed. In some cases, the reagents are finely powdered whereas in other cases, they are sintered to minimize their surface area and prevent uninitiated exothermic reactions, which can be dangerous. The synthesis is initiated by point-heating of a small part (usually the top) of the sample. Once started, a wave of exothermic reaction sweeps through the remaining material. SHS has also been conducted with thin films, liquids, gases, powder-liquid systems, gas suspensions, layered systems, gas-gas systems, and others. Reactions have been conducted in a vacuum and under either inert or reactive gases.

I. Synthesis Of Zinc Doped Lanthanum Ferrite

The self-propagating method is widely used in synthesis of ferrite nanocrystals because of its high reaction rate, low preparation temperature, and production of small particles. Hence, in present experiment, two preparations: Lanthanum Ferrite (LF) and Zinc doped Lanthanum ferrite (LZF) are synthesized. Citric acid $C_6H_8O_7$, Ferric nitrate $Fe(NO_3)_3 \cdot 9H_2O$, Lanthanum nitrate $La(NO_3)_3 \cdot 6H_2O$, Zinc nitrate $Zn(NO_3)_2 \cdot 6H_2O$ were produced by Merck company and were used as raw materials. The stoichiometric amount of nitrates and citric acid were dissolved separately in distilled water to make 0.1 M. The mole ratio of metal nitrates to citric acid was taken as 2:1. The ammonia solution was added into the solution to adjust the pH value to 7 and stabilize the nitrate-citrate solution.

During this procedure, the solution was continuously stirred using a magnetic agitator and kept at a temperature of 50 °C. Then, the mixed solution was poured into a dish, heated slowly to 100 °C and stirred constantly until the viscosity and colour changed as the solution turned into a brown porous dry gel. The dried gel simultaneously burnt in a self-propagating ignition manner until all the gel was completely burnt out to form a loose powder. The as-synthesized powders were then calcined at a temperature of 800 °C for 5 hrs.

III. RESULT AND DISCUSSION

Sol-gel self-ignition method is the simplest methodology to synthesize the nano-sized ferrites with good homogeneity at low annealing temperature. The lanthanum zinc ferrite nanoparticles are synthesized by sol-gel self-ignition method and characterized under the following techniques.

A. Structural Analysis

Fig.5.1 shows the X-ray diffraction of $\text{La}_x\text{Zn}_{1-x}\text{Fe}_2\text{O}_4$ ($x = 0.0 \leq x \leq 0.3$) samples. All the diffraction peaks can be indexed to the orthorhombic perovskite structure of $\text{La}_x\text{Zn}_{1-x}\text{Fe}_2\text{O}_4$ with lattice constants (Table 5.1) within a maximum experimental error of ± 0.0004 , which is in accordance with the bulk LaFeO_3 crystal (JCPDS 37-1493). The sizes of crystallites in the sample are evaluated by measuring the FWHM of the most intense peak (121). The results are shown in the Table 5.1 [1].

Table 5.1 2θ (121) values of Lanthanum Zinc Ferrite Samples

Samples	Grain size D (nm)	Lattice Parameter		
		(a) (Å)	(b) (Å)(c) (Å)	
LaFeO_3	40.933	5.555	7.8597	5.5598
$\text{La}_{0.9}\text{Zn}_{0.1}\text{FeO}_3$	44.423	5.5609	7.8591	5.5803
$\text{La}_{0.7}\text{Zn}_{0.3}\text{FeO}_3$	33.890	5.5570	7.8713	5.6541

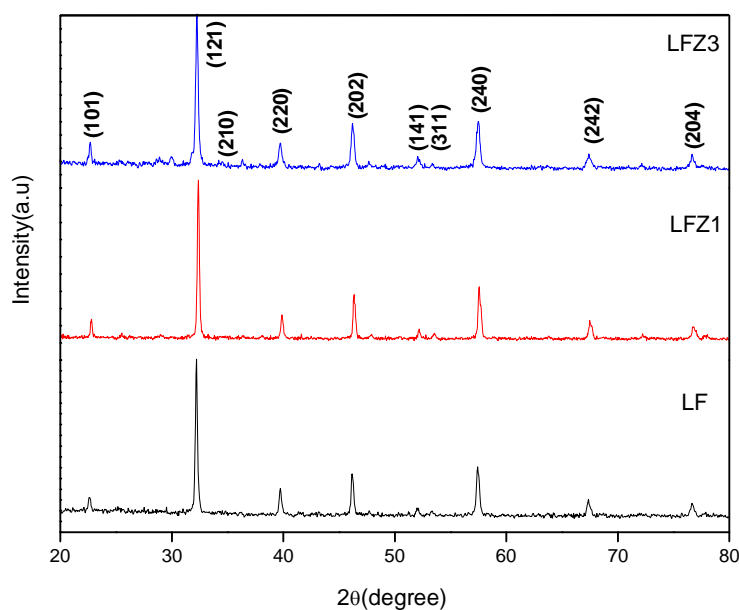
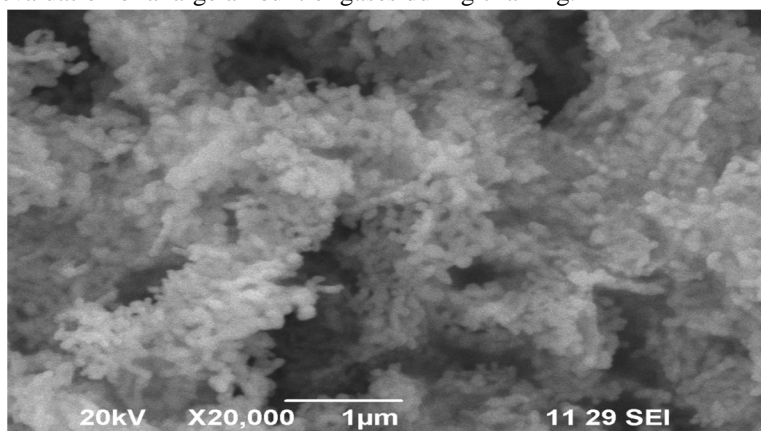


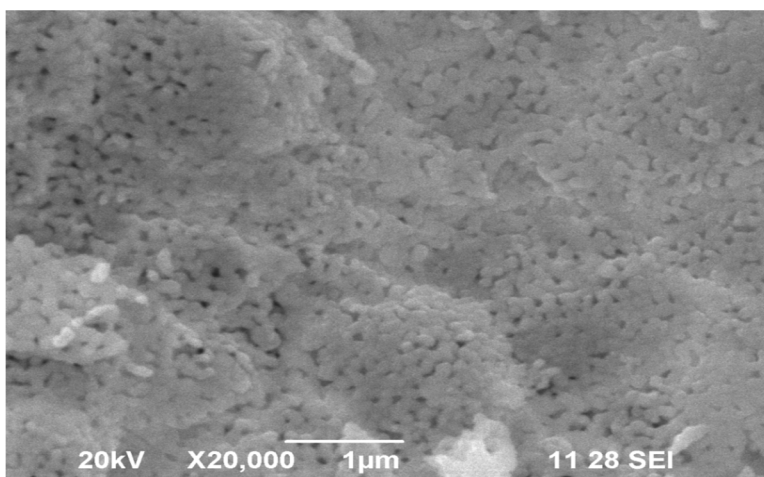
Fig. 5.1 XRD patterns of (a) LaFeO_3 (b) $\text{La}_{0.9}\text{Zn}_{0.1}\text{FeO}_3$ (c) $\text{La}_{0.7}\text{Zn}_{0.3}\text{FeO}_3$

B. Morphology Analysis

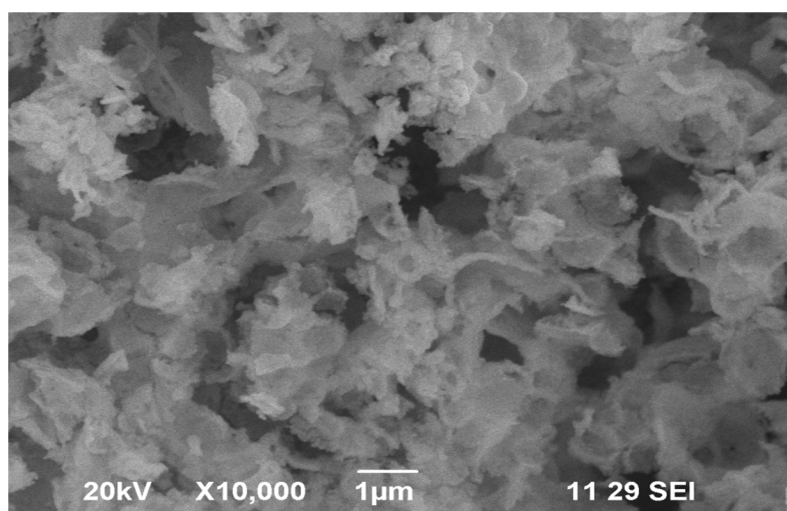
The surface morphology of the prepared samples was found to be different while increasing the zinc content. The SEM images are shown in Fig. 5.2. The Fig. 5.2 indicates that the nano-sized $\text{La}_x\text{Zn}_{1-x}\text{Fe}_2\text{O}_4$ is uniformly distributed and is composed of porous networks, which is due to the evaluation of a large amount of gases during charring.



(a)



(b)



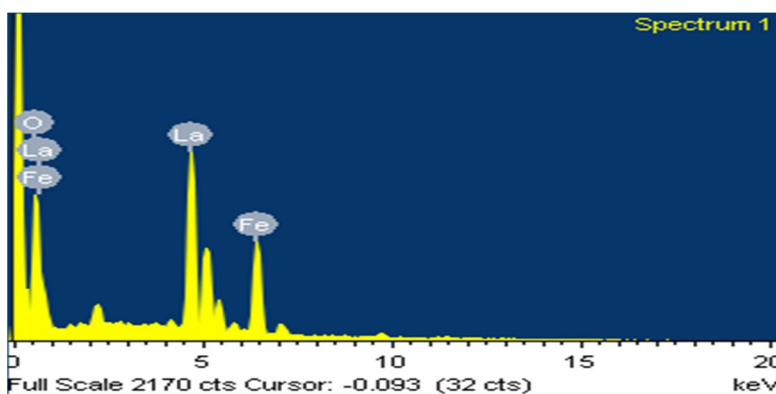
(c)

Fig. 5.2 SEM photographs of (a) LaFeO_3 (b) $\text{La}_{0.9}\text{Zn}_{0.1}\text{FeO}_3$ (c) $\text{La}_{0.7}\text{Zn}_{0.3}\text{FeO}_3$

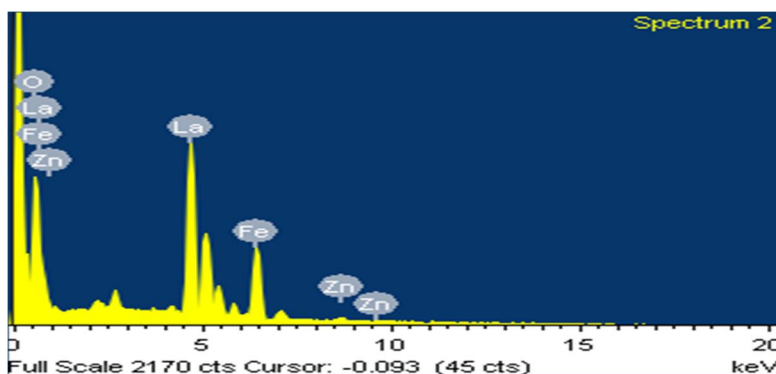
C. Compositional Analysis

The chemical compositions of $\text{La}_x\text{Zn}_{1-x}\text{Fe}_2\text{O}_4$ ($x = 0.0 \leq x \leq 0.3$) ferrite nanoparticles have been calculated by EDAX. Fig. 3 shows the EDAX pattern for the various compositions of ferrite nanoparticles. The peaks of the elements Fe, La, Zn and O were observed and have been assigned. The EDAX pattern confirmed the homogeneous mixing of the La, Fe, Zn and O atoms in pure and doped ferrite samples. The observed composition is almost equal to that of the sample produced by stoichiometric calculations.

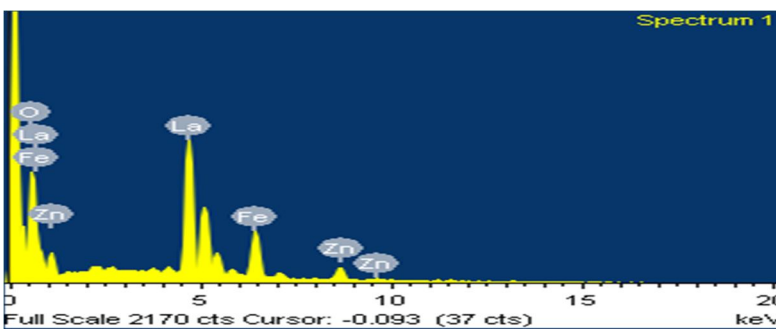
Elements present	LaFeO_3 (Wt %)	$\text{La}_{0.9}\text{Mg}_{0.1}\text{FeO}_3$ (Wt %)	$\text{La}_{0.7}\text{Mg}_{0.3}\text{FeO}_3$ (Wt %)
O	64.82	67.46	66.29
La	18.08	18.00	18.36
Fe	17.10	13.31	10.86
Zn		1.23	4.48



(a)



(b)



(c)

Fig. 5.3 EDAX photographs of (a) LaFeO_3 (b) $\text{La}_{0.9}\text{Zn}_{0.1}\text{FeO}_3$ (c) $\text{La}_{0.7}\text{Zn}_{0.3}\text{FeO}_3$

D. FTIR Analysis

Fig.5.4 the FTIR spectra for LaFeO₃ prepared by sol-gel self-ignition method. The broad band observed at 3400 cm⁻¹ is characteristic of the H-O bending mode of absorbed water or the hydrogen bonded to the oxygen ions in the framework. In addition, the band observed at 2924 cm⁻¹ corresponds to the physically absorbed CO₂ and the two bands 2357 and 1642 cm⁻¹ originate from the symmetric and asymmetric stretching of the carboxyl root. The smaller peaks at 1031 cm⁻¹ corresponds to the principle vibration of the CO₃²⁻ group due to the exposure to the ambient atmosphere, indicating that La species exist on the LaFeO₃ surface of the perovskite compound. In addition, the intense band at 557 cm⁻¹ can be attributed to the Fe-O stretching vibration being characteristic of the octahedral FeO₆ group in LaFeO₃.

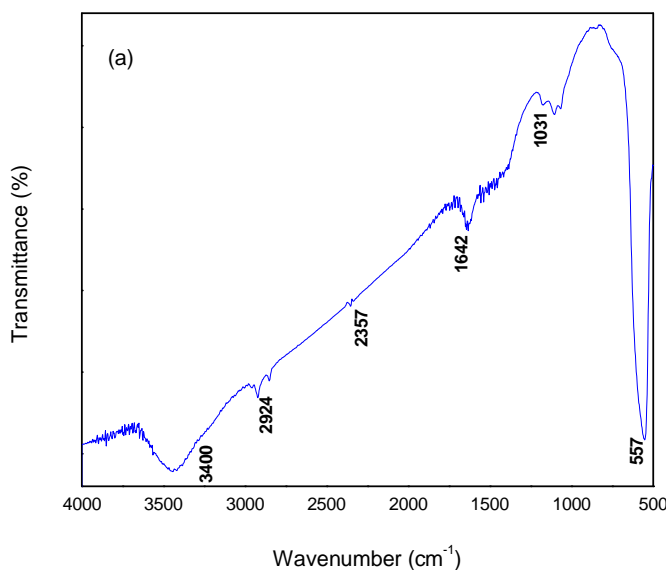
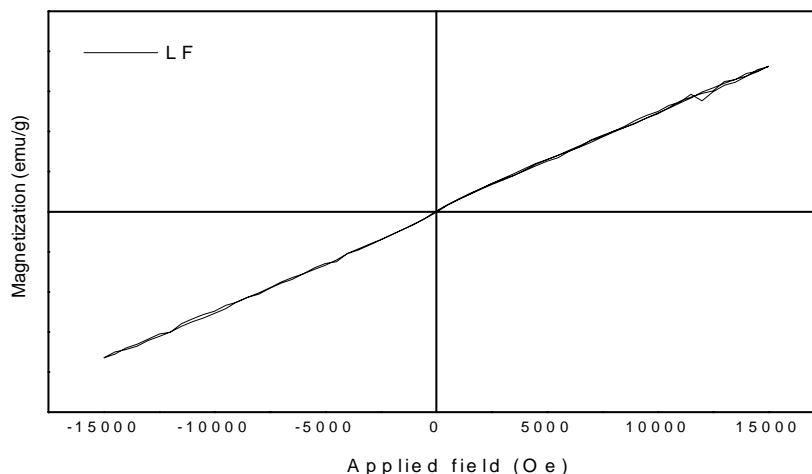


Fig. 5.4 FTIR spectras of (a) LaFeO₃

E. Magnetic Measurement Analysis

The magnetization versus applied field for different samples is shown in Fig. 5.5. The values of coercivity (H_c) and saturation magnetization (M_s) of all the samples are extracted from the loops. It is clear from Fig. 5.5 that the magnetization decreased with increasing Zn content. As the Zn content increases the particle size decreases. The existence of some degree of the spin canting in the whole volume of the nanoparticles and the disordered surface at the surface can explain the decrease of the saturation magnetization.



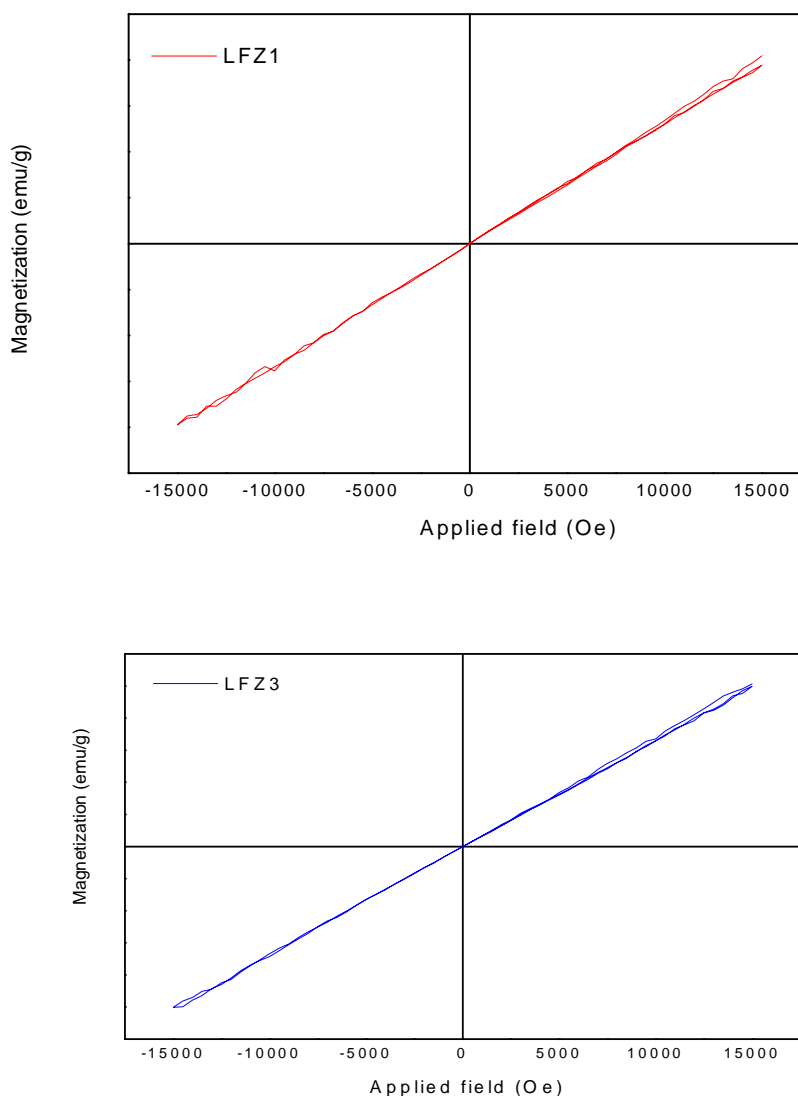


Fig. 5.5 M-H hysteresis curve of (a) LaFeO_3 (b) $\text{La}_{0.9}\text{Zn}_{0.1}\text{FeO}_3$ (c) $\text{La}_{0.7}\text{Zn}_{0.3}\text{FeO}_3$

IV. CONCLUSION

From this study the following results could be achieved. The following properties make the Zn-substituted Lanthanum ferrite suitable for some applications including photocatalysts, gas sensors applications which need a moderate saturation magnetization and particle sizes.

- A. All the diffraction peaks can be indexed to the orthorhombic perovskite structure of $\text{La}_x\text{Zn}_{1-x}\text{Fe}_2\text{O}_4$ which is in accordance with the bulk LaFeO_3 crystal (JCPDS 37-1493).
- B. The nano-sized $\text{La}_x\text{Zn}_{1-x}\text{Fe}_2\text{O}_4$ is uniformly distributed and is composed of porous networks, which is due to the evaluation of a large amount of gases during charring.
- C. No impurity peaks are observed from the EDAX analysis.
- D. The intense band at 557 cm^{-1} can be attributed to the Fe-O stretching vibration being characteristic of the octahedral FeO_6 group in LaFeO_3 .
- E. As the Zn value increases the particle size and magnetic ion concentration decrease, so that the saturation magnetization decreases.

REFERENCE

- [1] Oana Mihai, Steinar Raaen, De Chen and Anders Holmena, J. Mater. Chem. A, 2013, 1, 7006.
- [2] A. O. Merkushkin and Zaw Ye Maw Oo, Inorganic Materials: Applied Research, 2012, Vol. 3, No. 5
- [3] Z. S. Vinokurov, A. N. Shmakov, and V. A. Sadykov, Bulletin of the Russian Academy of Sci. Phy. 2013, Vol. 77, No. 2, pp. 138–141.
- [4] N. I. Solin, S. V. Naumov, and A. A. Samokhvalov, Phy. Solid State, Vol. 42, No. 5, 2000, pp. 925–930.
- [5] V. V. Parfenov, Sh. Sh. Bashkirov, A. A. Valiullin, and A. V. Averyanov, Phy. Solid State, Vol. 42, No. 7, 2000, pp. 1310–1312.
- [6] R. U. Mullai, P. Priyadharsini Pradeep, G. Chandrasekaran, Inter. J. Recent Trends in Sci. Tech, Volume 5, Issue 2, 2012.
- [7] N. Zhang, G. Srinivasan, A. M. Balbashov, J Mater Sci (2009) 44:5120–5126
- [8] E. Povoden-Karadeniz, A.N. Grundy, M. Chen, T. Ivas, and L.J. Gauckler, JPEDAV (2009) 30:351–366
- [9] P. C. Piña · R. Buentello · H. Arriola · E. N. Nava, Hyperfine Interact (2008) 185:173–177
- [10] Martin Søgaaard, Anja Bieberle-Hütter, Peter Vang, Hendriksen, Mogens Mogensen, Harry Louis Tuller, J. Electroceram (2011) 27:134–142
- [11] Pintu Sen, g. parravaxo, Inter. J. Mater, Methods and Tech Vol.1, No.1, PP: 01- 07,
- [12] P. C. Piña, R. Buentello, H. Arriola, E. N. Nava, Hyperfine Interact (2008) 185:173–177
- [13] A. O. Merkushkin, and Zo E Mo, Glass and Ceram, Vol. 68, Nos. 9 – 10,
- [14] Maxim V. Kuznetsov, Quentin A. Pankhurst, Ivan P. Parkinc, and Yury G. Morozova
- [15] Jiguangdeng, Hongxingdai, Haiyanjiang, Leizhang, Guozhiwag, Hong he, and Chaktongau, Environ. Sci. Technol. 2010, 44, 2618–2623
- [16] R. Andoulsi, K. Horchani-Naifer, M. Férid, Ceram. 58 (2012) 126-130
- [17] P.A. Desai and Anjali A. Athawale, Defence Sci. J. Vol. 63, No. 3,
- [18] Mahmoud Lebid and Mahmoud Omari Arab, J. Sci. Eng. (2014) 39:147–152
- [19] Wei Yang, Runduo Zhang, Biaohua Chen, Daniel Duprez, and Sébastien Royer
- [20] M. Sivakumar, A. Gedanken, W. Zhong, Y. H. Jiang, Y. W. Du, I. Brukental, D. Bhattacharya, Y. Yeshurunc and I. Nowikd
- [21] M. Küpferling, P. Novák, K. Knížek, M. W. Pieper, R. Grössinger, G. Wiesinger, and M. Reissner, J. App. Phy. 97, 10F309 (2005); doi: 10.1063/1.1855710
- [22] Ruifei Qin, Hongwei Song, Guohui Pan, Xue Bai, Biao Dong, Songhai Xie, Lina Liu, Qilin Dai, Xuesong Qu, Xinguang Ren, and Haifeng Zhao
- [23] C. Gueho, D. Giaquinta, J. L. Mansot, T. Ebel, and P. Palvadeaut, Chem. Mater. 1995, 7, 486–492
- [24] Marco Daturi and Guido Busca, Chem. Mater. 1995, 7, 2115–2126
- [25] Isabella Natali Sora, Tullio Caronna, Francesca Fontana, Cesarde Julia Fernandez, Andrea Caneschi, Mark Green, J. Solid State Chem 191 (2012) 33–39
- [26] Noppakun Sanpo, James Wang and Christopher C. Berndt, J. Australian Cer. Society Volume 49 [1], 2013, 84 – 91
- [27] Victor L. Kozhevnikov, Ilia A. Leonidov, Julia A. Bahteeva, Mikhail V. Patrakeev, Edward B. Mitberg, and Kenneth R. Poeppelmeier, Chem. Mater. 2004, 16, 5014–5020
- [28] Christopher M. Kavanagh, Richard J. Goff, Aziz Daoud-Aladine, Philip Lightfoot, and Finlay D. Morrison
- [29] Marta Maria Natile, Andrea Ponzoni, Isabella Concina, and Antonella Glisenti
- [30] Xiao Ping Dai, Qiong Wu, Ran Jia Li, Chang Chun Yu, and Zheng Ping Hao, J. Phys. Chem. B 2006, 110, 25856–25862



10.22214/IJRASET



45.98



IMPACT FACTOR:
7.129



IMPACT FACTOR:
7.429



INTERNATIONAL JOURNAL FOR RESEARCH

IN APPLIED SCIENCE & ENGINEERING TECHNOLOGY

Call : 08813907089  (24*7 Support on Whatsapp)